



## Research article

# Co-optimisation of wind and solar energy and intermittency for renewable generator site selection

Hao Wu\*, Samuel R. West

CSIRO, 10 Murray Dwyer Cct, Mayfield West, 2304, New South Wales, Australia

## ARTICLE INFO

Dataset link: <http://www.bom.gov.au/research/projects/reanalysis/>

## Keywords:

Renewable generation site selection  
Resource assessment  
Multi-objective optimisation  
Solar farm  
Wind farm  
Australia

## ABSTRACT

Sites for the construction of wind and solar farms have typically been chosen to maximise total energy generation of an individual site, but rarely consider the intermittency of the renewable resource available at each location. As more renewable generation is added to electricity grids around the world, this intermittency is rapidly becoming a major factor constraining the volume of renewable generation that can be added cost-effectively, as additional fast-response storage or dispatchable generation must compensate for periods of low renewable generation. We present a statistical approach to selecting wind and solar generation sites that assesses energy and intermittency of individual wind, solar and co-sited wind plus solar farm locations, allowing energy and intermittency to be given weight when selecting sites for new generation. A new multi-objective pareto-front approach to identifying high-performing renewable generation sites that allows for optimising multi-site selection using the median (energy) and median absolute difference (intermittency) of historical weather resource is proposed. This technique is then applied to a 30-year, hourly, Australian weather reanalysis dataset to show the potential improvement over the fleet of wind and solar farms currently operating in the Australian National Energy Market. Finally, an analysis of potential sites for optimal offshore wind and combined offshore wind and solar is presented. The proposed wind-only and solar-only sites show an average energy increase of 9% (solar, 67 sites), 28% (wind, 50 sites) more energy for the same level of intermittency, as compared to the existing generation sites. Three existing combined wind and solar sites were compared to the best three proposed sites, which showed a 3-16% energy increase for the same intermittency, or a 2-11% intermittency decrease for the same energy generated.

## 1. Introduction

With advancements in technology and the rapid global economic growth, natural resources are being consumed at an alarming and unsustainable rate. According to UN Environment's Global Resources Outlook 2019, fossil fuel use has increased by 45% along with more than tripled resource extraction since 1970, which leads to growing urgency around climate change concerns. Worldwide, greenhouse gases emissions from human activities increased by 43% from 1990 to 2015 (US Environmental Protection Agency). The Intergovernmental Panel on Climate Change (IPCC) reported that under all scenarios examined, Earth is likely to breach the crucial

\* Corresponding author.

E-mail address: [helen.wu@csiro.au](mailto:helen.wu@csiro.au) (H. Wu).<https://doi.org/10.1016/j.heliyon.2024.e26891>

Received 27 July 2023; Received in revised form 29 January 2024; Accepted 21 February 2024

Available online 27 February 2024

2405-8440/© 2024 The Author(s). Published by Elsevier Ltd. This is an open access article under the CC BY-NC-ND license (<http://creativecommons.org/licenses/by-nc-nd/4.0/>).

## Australian electricity generation renewable sources

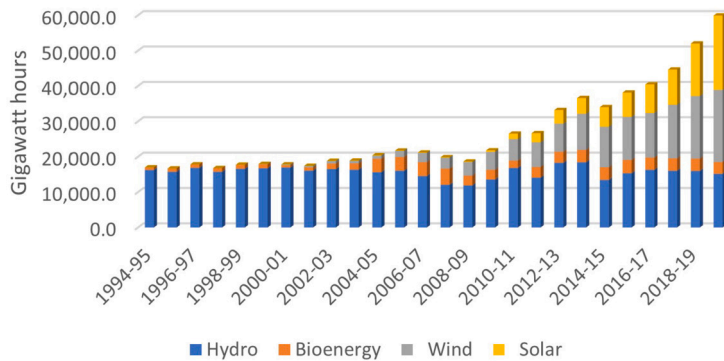


Fig. 1. Australian Renewable Generation by Type.

1.5 degree Celsius climate threshold by 2027. Under the Paris Agreement countries pledged to limit global warming to well below 2 degrees Celsius, which requires urgent action to cut CO<sub>2</sub> and other greenhouse gas emissions in the coming decades.

In the meantime, renewable energy is produced using natural resources that are constantly replenished. It is also associated with reduced carbon footprint, for example, the carbon footprint of solar and wind are many times lower than coal or gas with carbon capture and storage (CSS) even after accounting for emissions during manufacture, construction and fuel supply. Therefore, renewable energy as an alternative has played an increasingly prominent role in the transition towards low carbon emissions. Australia pledged to reduce emissions by 26% to 28% below the 2005 level by 2030 and therefore requires high penetration of renewable energy in the power system.

In Australia, renewable resources are abundantly available and widely distributed across the country. Fig. 1 shows the electricity generation from renewable resources has risen by 126% in Australia over the last 10 years. Australia has a diversified profile of renewable energy as wind and solar have been the primary driver in renewable generation expansion, with the share of hydro stabilized. A Renewable Energy Target (RET) scheme was introduced in 2001 to ensure that 20% share of renewable source in electricity generation by 2020 and Australia met its 2020 renewable energy target in 2019. As many of the Australian states and territories have set ambitious goals for renewable energy expansion by 2030, solar and wind power plants are being planned and developed at an accelerating rate. Hydro power was the largest source of renewable energy in Australia before 2019, however, it is not discussed in detail here due to its lower potential for increased capacity. In this project, we focus on wind and solar energy as they currently generate a larger share of renewable energy. In 2020, wind power took 35.9% share of renewable electricity and 9.9% of total electricity in Australia, whereas solar power took the second-largest share of electricity production for renewable energy, 35.78% of renewable electricity and 9.9% of total electricity. As at the end of 2021, solar PV installations had a combined capacity of 25,321 MW of which 4,613 MW were installed in the previous year.

With continued renewable energy expansion in Australia, most of the projects focus on stand-alone wind or solar farms. Variability and intermittency are the intrinsic nature of wind and solar resource, see [1]. Variability is a measure of change on a regular daily or longer temporal basis, while intermittency measures random changes due to different weather conditions. Wind power varies on a daily basis and it is also considered highly intermittent because its output depends on wind speed, atmospheric conditions and other factors. Solar power depends on slower-changing cloud cover so it less intermittent than wind in most cases. The intermittent nature of wind and solar resources imposes challenges on grid operators to determine the available amount of power at a given moment.

Wind and solar power generation can be complementary since they are generated by different renewable resources which are often negatively correlated. We can take advantage of this by building wind and solar generators in select locations such that their aggregate becomes less intermittent than their individual power output. A steadier power supply helps improve predictability and operability of the electrical grids, ultimately making high renewable penetration levels easier and cheaper to achieve.

The research of combined solar and wind power grows actively from a global perspective. The most recent literature review conducted by [2] has shown that research on solar and wind complementarity has been undertaken in all continents except Africa and Antarctica. Most of the studies investigated the correlation between wind and solar for a limited number of locations, while some of them provide a more general assessment of wind and solar complementarity in a specific territory.

In Europe, [3] analysed the correlation between large-scale wind and solar power in Sweden and the results showed that wind and solar power are negatively correlated from hourly to annual time scale. The analysis of co-located solar and wind power generation project has shown that hybrid systems in general produce more reliable electricity and is preferable to stand-alone systems. [4] showed a potentially strong negative correlation between solar and wind resources at the monthly scale in the Iberian Peninsula. A strong monthly negative correlation coefficient of wind and solar has been confirmed by [5] based on a sample year in Italy. [6] investigated the daily co-variability of wind and solar in Britain and considered the variability in the total power output of wind and solar power systems. Their findings suggested that daily variability in total generated power is always reduced by incorporating solar. A continental-scale study has been conducted by [7] to assess the reliability of a combined use of solar and wind

energy over Europe. A degree of local negative correlation between wind and solar is apparent in many regions for hourly data. [8] extended the analysis to offshore wind and solar resources and identified areas with high potential and low variability in the Mediterranean. It also highlighted the advantages of combined wind and solar at selected locations in terms of increased monthly energy production.

In North America, the smoothness of energy production, which is defined as decreased instances of both high and low values in power generation as compared to the generation by individual resource, has improved when combining solar and wind as compared to stand-alone systems in selected locations in Ontario, see [9] for details. In the USA, the complementarity of wind and solar resources has been investigated in various regions of Texas. [10] found that the strongest negative correlation of wind and solar exhibits on daily and annual levels based on half-hourly power production. Strong complementarity appears when pairing West and South Texas wind power. It also suggests that combination of wind and solar can make renewable energy production more reliable in Texas.

In South America, [11] represented complementarity of wind and solar in the form of maps for the state of Rio Grande do Sul, in southern Brazil. The results indicate that for some areas of the state hybrid wind-solar power systems could be more effective than single photovoltaic or wind systems.

In Asia, [12] showed that combining different resources improves smoothness in power output when compared to each source in China. In the hourly time scale, there is also a smoothing effect of combining the spatially dispersed wind power systems when the dispersion of sites is large enough. [13] adopted the copula approach to characterize the dependence structure between wind and solar. It found that the wind-solar complementarity is stronger in the northwestern and northern regions of China.

In Australia, quantitative research has been undertaken to analyse solar and wind complementarity and interaction. [14] investigated the correlation of wind and solar resources using hourly weather data, however, their analysis was limited to a single site in New South Wales. Recently, the study of spatial and temporal complementarity of wind and solar resources in Australia was pioneered by [15] using the Modern Era Retrospective Analysis for Research and Application (MERRA) climate reanalysis data for the period 1979-2014. The results have shown that the generation of solar and wind hybrid systems could be maximized along the western and southern coast of Australia and wind and solar power intermittency can be best mitigated by the synergy of wind and solar resources within a distance of about 465 km.

For the publications mentioned above, correlation coefficients are extensively used to characterise the strength of complementarity between wind and solar resources, see, for example, [14], [3], [12], [5], [6], [7], [10] and [13]. In the meantime, standard deviation and coefficient of variation are adapted in a great extent to quantify the variability in the underlying data, see [12], [4] and [6]. The traditionally used complementarity and variability measures present a few limitations. Correlation coefficients only uncover relationships. Negative correlation suggests complementarity while positive correlation indicates synergy between the renewable resources. Standard deviation and coefficient of variation are sensitive to the presence of outliers or for the underlying distribution with long tails. Therefore, different measurement metrics are proposed in the literature, for example, relative coefficient of variation and interquartile range by [15]. [11] implemented three complementarity indices, i.e. Amplitude-related partial complementarity index, Time-related partial complementarity index and Total complementarity index, which are based on the range of available energy of two resources. [13] used copulas to construct the joint distribution of wind and solar energy so that Kendall's  $\tau$  correlation coefficient calculated is more accurate.

It is important to note that all the metrics in the literature to date only provide useful information on the correlation between two renewable resources. However, our research objective should be twofold; it is imperative to also quantify the relationship between variability and energy of the combined renewable energy output. For example, a location with a high negative correlation between wind and solar generation may still be undesirable if its total energy generation is very low. Single-objective metrics focused on correlation alone will not help distinguish poor vs. high-performing sites at the same correlation level, and so can give very misleading results. To address this issue, we propose a novel Pareto-frontier based method of evaluating renewable site selection using the dual metrics of energy and intermittency. With more recent and higher resolution data, more detailed studies are required to assess the intermittent nature of wind and solar, and their complementary in further detail using this new method. This study aims to explore the possible co-location of wind and solar farms and to provide a summary of large-scale wind and solar power synergy analysis. While this approach is applicable worldwide, in this paper we focus on Australia using long-term climatic hourly data for the period of 1990 to 2019 with a grid resolution of 12 km, whereas the MERRA product has a  $1/2^\circ$  (latitude, around 56 km) and  $2/3^\circ$  (longitude, 88-104 km in Australia) resolution. Moreover, it is desirable to provide useful information to developers who are considering co-locating developments to make well-informed decisions. We apply the Pareto-frontier method to identify the best grid points by examining the trade-off between median generated energy and the intermittency of supply available. This approach also allows direct numerical comparison of the best proposed sites with existing wind and solar farms in terms of energy and intermittency and calculation of potential improvements over standard site selection techniques.

## 2. Methodologies

### 2.1. Data

This project uses the Bureau's Atmospheric high-resolution Regional Reanalysis for Australia (BARRA) data. BARRA provides gridded data over a large region covering Australia from January 1990 to February 2019, using a weather model based on Australian Community Climate and Earth Simulator System (ACCESS) framework, see [16] for details. A total of 255624 hourly data were extracted from BARRA-R product for the period of 1st January 1990 to 28th February 2019 over Australia for our analysis. BARRA-R

provides 12 km spatial grids, which is higher resolution than other reanalysis data sets for this region. For example, it offers a higher resolution than the MERRA's  $1/2^\circ$  (latitude)  $\times$   $2/3^\circ$  (longitude) resolution and similar to MERRA data BARRA's model extends over 70 levels up to 80 km into the atmosphere. For the purpose of this study, the BARRA parameters used are the net radiant flux received by a surface per unit area ( $av\_netswsc$ ,  $W/m^2$ ), wind speed measured at the height of 10 m ( $av\_uwnd10m$ ,  $m/s$ , and  $av\_vwnd10m$ ,  $m/s$ ).

- Solar irradiance

Assessment of surface shortwave net radiation flux is essential for solar energy applications. The most relevant parameter from BARRA-R product is  $av\_netswsc$  ( $W/m^2$ ), which is the net downward shortwave radiation at the surface (ground or ocean surface).

- Wind Power

Wind resource assessment is based on the wind speed measured at the height of 10 m, which can be found in BARRA-R as parameters  $av\_uwnd10m$  (u-component) and  $av\_vwnd10m$  (v-component). Wind speed is calculated using the following Formula (1):

$$\text{wind speed}(w) = \sqrt{u^2 + v^2} \quad (1)$$

However, wind power density (WPD) is preferable since it better approximates the amount of wind energy ( $W/m^2$ ) available at a site for a wind turbine and is proportional to the wind speed. Furthermore, it is the essential component for calculating the total energy at a given site. WPD can be calculated as Formula (2):

$$\text{WPD} = \frac{1}{2} \rho w^3 \quad (2)$$

where  $\rho$  is the air density which was kept constant at a value of  $1.225 \text{ kg/m}^3$ .

## 2.2. Statistical analysis

In the literature, the complementarity of wind and solar resources has been quantified and evaluated by means of statistics and other indices. For this section, we assume paired data  $\{x_{t_1}^s, y_{t_1}^s, \dots, x_{t_n}^s, y_{t_n}^s\}$ , where  $x_t^s, y_t^s$  are time series from two resources (wind and solar) at location  $s$ . The superscript  $s$  could differ to represent different locations for later use. The subscript  $t$  indicates the timestamp of the observation, typically given in hours. The metrics adapted in this study are the following:

- **Correlation** Correlation is the most commonly used measure of dependence in a bivariate analysis. It quantifies the strength of association between two variables and the direction of the relationship. There are three frequently used correlations: Pearson's, Kendall's, and Spearman's correlation, where the first one is a parametric method and the latter two are non-parametric approaches. There are relatively strict assumptions for using Pearson correlation. It requires both variables to be continuous and approximately normally distributed, which indicates that it might not be an appropriate metric to measure the relationship between wind speed and solar irradiance data, since the previous studies suggest that wind speed and irradiance data do not follow normal distribution. For instance, [17] analysed the wind energy potential of the location at the southern region of Turkey based on Weibull and Rayleigh distribution, while [18] proposed a hybrid Beta-kernel density estimation model for solar irradiance probability estimation. Kendall's and Spearman's correlation are non-parametric methods that measure a monotonic relationship using ranked data. The distribution of raw data can be transformed more evenly by assigning ranks and the Spearman's correlation is obtained by calculating the Pearson's correlation from the ranks. Kendall's correlation is calculated based on concordant and discordant pairs. In most cases, Kendall correlation is more robust and efficient than Spearman's correlation and its interpretation of conformity is straightforward. Therefore, the Kendall's Tau was adapted and calculated in our study. Let  $(x_{t_1}^s, y_{t_1}^s), \dots, (x_{t_n}^s, y_{t_n}^s)$  be a set of paired random variables, any pair of observations  $(x_{t_i}^s, y_{t_i}^s)$ , and  $(x_{t_j}^s, y_{t_j}^s)$ , where  $t_i < t_j$ , are concordant if either both  $x_{t_i} > x_{t_j}$  and  $y_{t_i} > y_{t_j}$  holds or both  $x_{t_i} < x_{t_j}$  and  $y_{t_i} < y_{t_j}$ ; otherwise they are discordant. The Kendall's  $\tau$  coefficient is defined as in Formula (3):

$$\tau(x^s, y^s) = \frac{n_c - n_d}{n(n-1)/2}, \quad (3)$$

where  $n_c$  = number of concordant pairs,  $n_d$  = number of discordant pairs, and  $n$  = number of pairs. The hourly, daily, and monthly wind and solar outputs at each grid point are modelled based on the 29 years' reanalysis data. Fig. 2 and Table 1 show the Kendall's Tau correlation coefficient between wind and solar across Australia at various temporal scales. It is shown that solar and wind power could be negatively correlated on all temporal scales, from hourly to annual, and the negative correlation is at its maximum on a monthly scale.

The hourly wind and solar power shows the weakest correlation from  $-0.22$  to  $0.46$ , see Table 1. The hourly wind and solar power time series are aggregated into daily and monthly time series to assess the complementarity of wind and solar power on daily and monthly scale. The correlation of wind and solar is strongest on monthly scale with the minimum  $-0.54$  and maximum  $0.76$  while the minimum is  $-0.31$  and maximum  $0.44$  on daily scale. In terms of maximising renewable grid penetration, daily and hourly correlations are the most important, as these roughly correspond to grid dispatch, and energy storage time-frames, so minimising intermittency here has the most benefit to the grid.

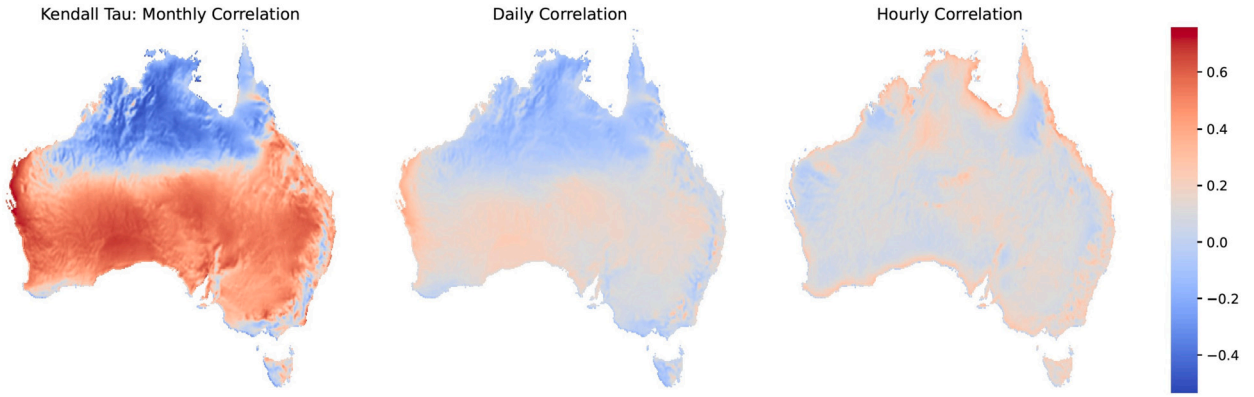


Fig. 2. Wind and Solar Correlation.

**Table 1**  
Summary table of correlation.

Kendall's Tau	hourly	daily	monthly
mean	0.12	0.07	0.25
std	0.06	0.11	0.33
min	-0.22	-0.31	-0.54
25%	0.08	-0.02	-0.03
50%	0.11	0.10	0.39
75%	0.15	0.15	0.53
max	0.46	0.44	0.76

In general, northern Australia, south-eastern and south-western coastal region and eastern Tasmania show strong negative correlation of wind and solar output on longer time scales, which suggests they are good spots for co-sited wind and solar. For short-term correlation, the pattern of correlation bears some resemblance to the topography of Australia, as shown in Fig. 3. It is possibly due to different diurnal patterns of the wind at various elevation levels. Strong surface heating during the day leads to turbulence in the lower levels and diurnal variation of wind. As a result, wind speed at lower level usually reaches its peak in the early afternoon due to the increased thermal instability of the atmospheric boundary layer, which is consistent with the profile of solar radiation. Therefore, positive correlations are observed in the Central Lowland and Coastal Plains. At the upper level, the trend is reversed and the wind speed during daytime is less than nighttime, which is opposite to the diurnal profile of solar radiation, and therefore, complementarity of wind and solar can be observed in Western Plateau and Eastern Highland regions.

- **Wind and Solar Complementarity and Synergy** To address three scenarios in this section, threshold values of power density of wind and solar are derived from historical data. For wind resource,  $WPD = 100W/m^2$  is used based on wind classification statistics, i.e.,  $100W/m^2$  is considered as poor wind power class at 10 m with the corresponding wind speed  $< 4.4m/s$ . For solar resource, the theoretical minimum is  $0W/m^2$ , however, considering the low efficiency of PV modules when GHI value falls below some threshold value,  $170W/m^2$  is used after calculating the lower quartile of all available GHI values for the BARRA dataset over Australia.

Let  $NOH$  denote the number of hours and  $TNOH$  denote total number of hours:

- Wind Complements Solar (WCS): Similar to the WCS defined in [15], this statistic describes the fraction of the time when wind resource is abundant while the solar farm is at a non-generating mode.

$$WCS = \frac{NOH(WPD > 100W/m^2 \& GHI \leq 170W/m^2)}{TNOH} \quad (4)$$

- Solar Complements Wind (SCW): This statistic represents the percentage of the time when solar resource is abundant while the wind farm is at a non-generating mode.

$$SCW = \frac{NOH(WPD \leq 100W/m^2 \& GHI > 170W/m^2)}{TNOH} \quad (5)$$

- Wind Solar Synergy (WSS): This statistic calculates the percentage of the time when either a solar farm or a wind farm is available at the same location.

$$WSS = \frac{NOH(WPD > 100W/m^2 \text{ XOR } GHI > 170W/m^2)}{TNOH} \quad (6)$$

Using Formula (4), (5) and (6), WCS, SCW and WSS were calculated based on 255624 hourly BARRA data for the period of 1st January 1990 to 28th February 2019 for each grid point within Australia. Fig. 4 shows three scenarios of solar and wind

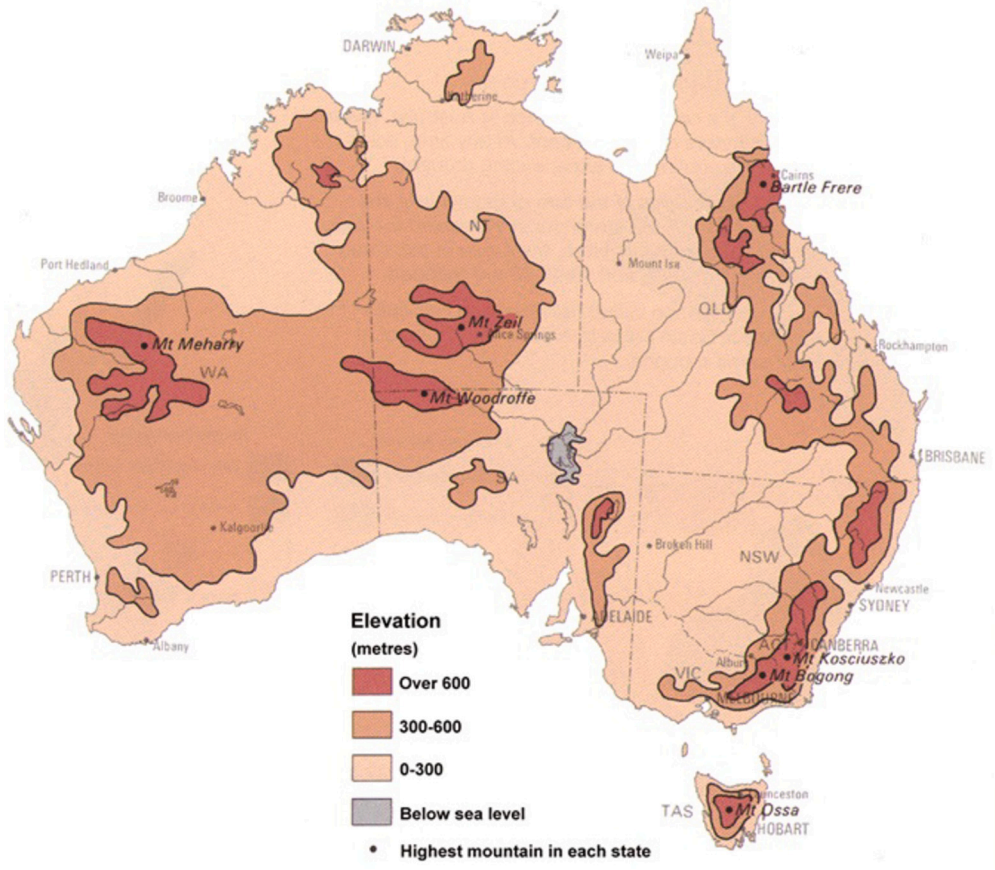


Fig. 3. Topographic Map of Australia.

synergy in Australia. It is clear that WCS in southern regions of Australia with top 100 locations coloured in green along the western, south-western and southern coastal areas. The northern and eastern regions show the lowest WCS of around 10%. For SCW, the opposite patterns have been observed. Northern and eastern regions show the highest SCW of around 35% with top locations are identified in Northern Territory and northern part of Queensland. The WSS ranges from 5% to 30% with the overall pattern similar to what has been observed in WCS. The northern and eastern regions shows the lower WSS while the western and southern regions shows the higher WSS. The top 100 locations in terms of WSS can be observed in the western and southern coastal regions.

- **Coefficient of Variation** The coefficient of variation, also known as relative standard deviation, measures the relative dispersion of data points around the mean. It is defined as the ratio of the standard deviation  $\sigma$  to the mean  $\mu$  as in Formula (7):

$$c_v = \frac{\sigma}{\mu}. \tag{7}$$

This metric can be used to assess the variability of wind and solar resources, separately and jointly. However, as it has been shown that wind speed and solar irradiance data are not normally distributed but rather very skewed, a modified coefficient of variation with reference to the median was introduced by [19] and is known as Relative Coefficient of Variation (RCoV).

- **Relative Coefficient of Variation** The RCoV is more suited to assessing distributions with extreme values, which could be observed in wind speed data. The calculation of RCoV is defined as follows:

$$RCoV = \frac{\text{median}|x_t^s - \text{median}(x_t^s)|}{\text{median}(x_t^s)} \tag{8}$$

The RCoV in Formula (8) is the ratio of absolute deviation about the median to the median and it is less sensitive to the extreme values which are commonly observed in wind and irradiance data. If two locations are considered for development of renewable energy and they have the same power density, the one associated with a lower RCoV is preferred since it will produce a more constant power generation. The RCoV was employed as a main metric for evaluating the variability of wind and solar resources across the Australia continent by [15]. In their study, however, the RCoV was calculated for wind and solar power density separately. As the synergy characteristic is the main concern for co-location projects and it is desirable to have stable power output with less variability, the hourly RCoV of the *sum* of wind and solar resources provides more information to serve this purpose.

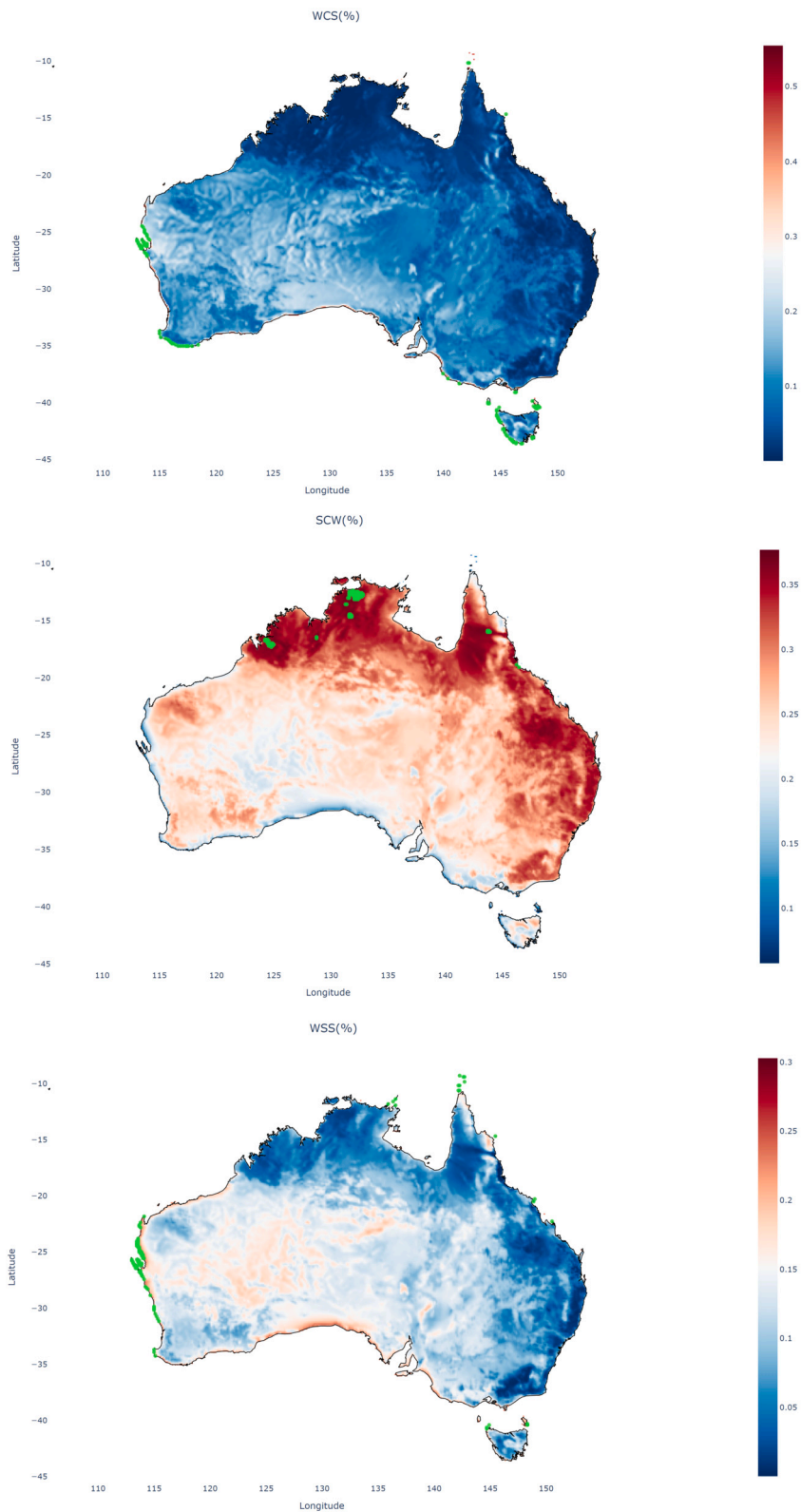


Fig. 4. Wind Complements Solar, Solar Complements Wind and Wind and Solar Synergy in Australia. Green dots show the top 100 locations in terms of Wind-Solar Synergy (WSS).

### 3. Results and analysis

#### 3.1. RCoV of solar, wind and combination of solar and wind

Fig. 5 shows the RCoV of solar, wind and combination of wind and solar resources in Australia.

The RCoV of solar resource is calculated by filtering out the night hours when the PV power output is negligible. Since the RCoV is the ratio between median absolute deviation and median, a lower RCoV indicates lower variability when medians are the same or higher median output when the variability are the same. As geography affects solar energy potential and areas that are closer to the equator have a higher amount of solar radiation, it is expected to observe higher RCoV in southern regions and gradually decreasing as it moves towards the equator.

For wind resource, large RCoV values ( $> 0.9$ ) can be observed in east coast, northwest coastal regions and Tasmania. It shows the reduced RCoV in Western Plateau at around 0.75 and reaches it minimum of 0.6 in the Central Lowland.

The complementarity between wind and solar at each grid point are assessed by calculating the RCoV of wind and solar at the same location. The third figure of Fig. 5 shows the RCoV of wind power density and solar irradiance across Australia. RCoV of wind and solar can be considered as a measure of temporal synergy of solar and wind in Australia to understand the complementarity characteristic of the resources. As it is important to ensure power grids have consistent coverage from wind and solar, the night hours solar data are not filtered out but summed with wind data to produce continuous output of the renewable resources. For the onshore regions, the RCOVs are generally between 0.8 and 1, which indicates that the complementarity between wind and solar is uniformly distributed across Australia continent. However, there are regions along Great Dividing Range of east coast and in Kimberley Plateau of northern Western Australia have larger values of RCoV, which is close to 1. It suggests that with the same median absolute deviation those sites provide smaller median flux of energy and with the same median flux of energy those sites would have larger median absolute deviation, i.e., the intermittency. Therefore, they are not preferable if the co-location of wind and solar projects are considered. On the contrary, sites along southwest WA coastal areas have RCoV value close to 0.6.

RCoV shows the extent of variability in relation to the median. However, RCoV itself is not a good metric to select wind and solar farm sites. The site selection process should be a multi-objective optimization since at each median absolute deviation value, the grid point with the largest median is optimal and at each median value, the grid point with the smallest median absolute deviation is optimal. It is desirable to restrict attention to the set of efficient choices, and to make trade-offs within this set.

#### 3.2. Pareto frontier & RCoV

To select good locations to co-site complementary wind and solar generation, the major considerations are the amount of energy (the median) generated and the intermittency of that energy (the RCoV). These two objectives are visualised using scatter plots, and the optimal sites (those 'closest' to the top-left corner) form a pareto-front - that is, the set of sites which have the best combination of these two traits. Selecting from the pareto set required a further subjective value judgement to be made using external context, for example, do we prefer sites with a good balance between energy and intermittency, or is just maximising energy at higher intermittency levels preferable? In this section we present results and analysis to help identify the pareto-optimal locations.

To further analyse the optimal profiles of wind and solar, the scatter plot of median vs. median absolute difference has been produced. In order to identify the set of efficient choices, the Pareto frontier is calculated and marked in Fig. 6. The Pareto frontier or Pareto set is the set of all Pareto-efficient situations. It can be more formally defined as follows. Consider a system with function  $f : X \rightarrow \mathbb{R}^m$  where  $X$  is a compact set of feasible decisions in the metric space  $\mathbb{R}^n$ , and  $Y$  is the feasible set of criterion vectors in  $\mathbb{R}^m$ , such that

$$Y = \{y \in \mathbb{R}^m : y = f(x), x \in X\}.$$

We assume that the preferred directions of criteria values are known. A point  $y'' \in \mathbb{R}^m$  strictly dominates another point  $y' \in \mathbb{R}^m$ , written as  $y'' > y'$ . The Pareto frontier  $P(Y)$  is written as:

$$P(Y) = \{y' \in Y : \{y'' \in Y : y'' > y', y' \neq y''\} = \emptyset\}.$$

Depending on the preferred directions of criteria values, points on the frontier dominate points off the frontier. In Fig. 6, the multi-objective optimisation can be specified as maximising the median (energy output) while minimizing the median absolute difference (the variability/risks). The points on the frontier (red) are said to 'dominate' the ones off the frontier (blue) because for a given frontier point, any other points with the same variability gives lower energy output or have the same energy output but higher median absolute difference, and so on.

The first scatterplot in Fig. 6 shows median vs. median absolute deviation of wind power density for all grid points in Australia with the existing solar farms in green and the Pareto frontier in red. The plot suggests that there are better options of sites than the existing wind farms given that the green points are dominated by the Pareto frontier in red. The second scatterplot shows the RCoV profile of solar and it seems to be more volatile than that of the wind given the spread of points are much wider. The distance between Pareto frontier and the existing solar farms is notable and is approximately  $80 W/m^2$ . As there are no existing co-location of wind and solar farm, the third scatterplot shows the Pareto frontier and all grid points. It suggested that the power output could be much promising if we choose a site from Pareto frontier rather than selecting it randomly.

The Pareto frontiers of wind, solar, and wind plus solar in Australia are identified and marked in green in maps of Fig. 7. For solar resource, the Pareto frontiers generally form three clusters, two in Northern Territory and one in Tasmania. It is clear that the

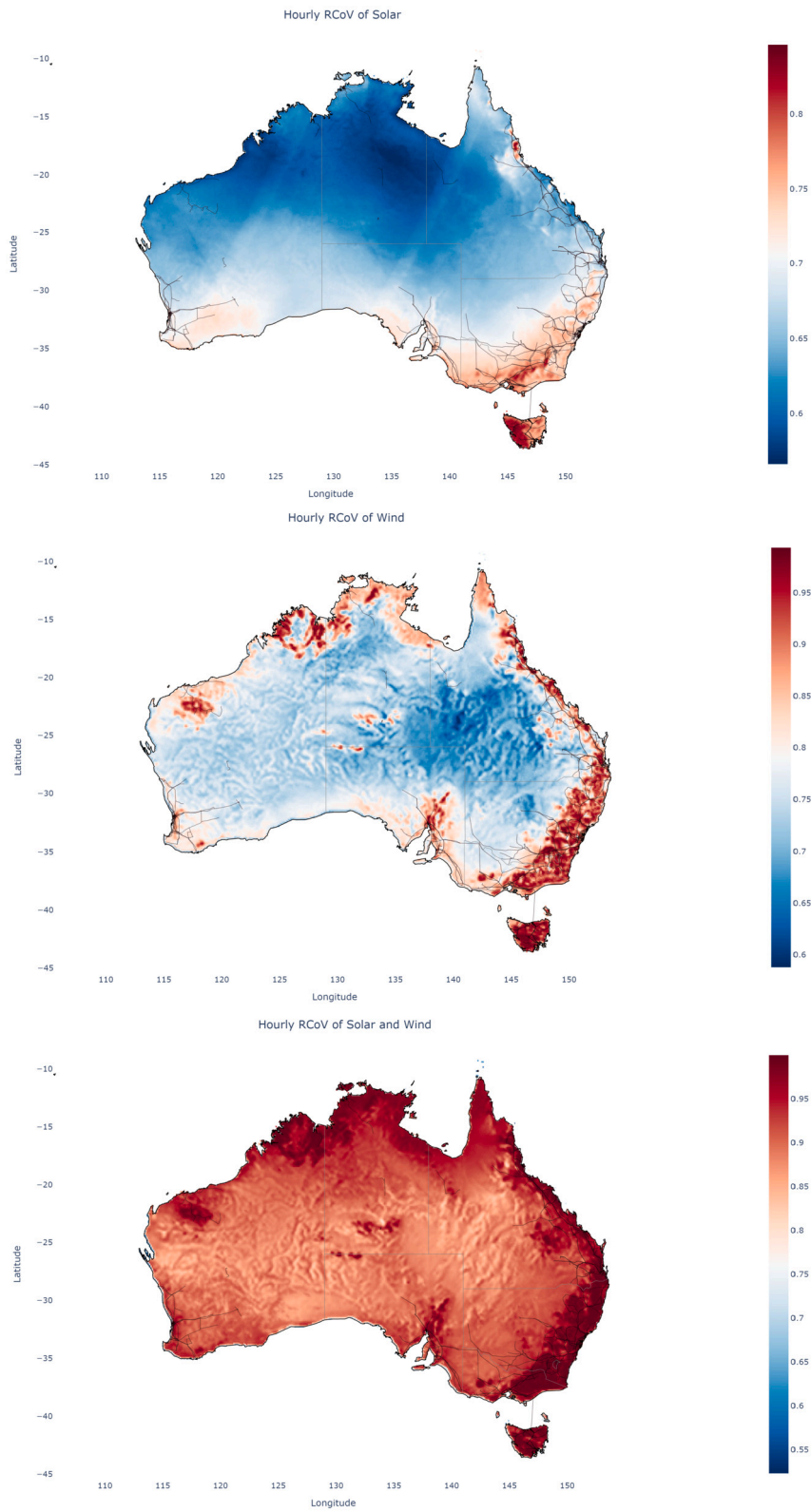
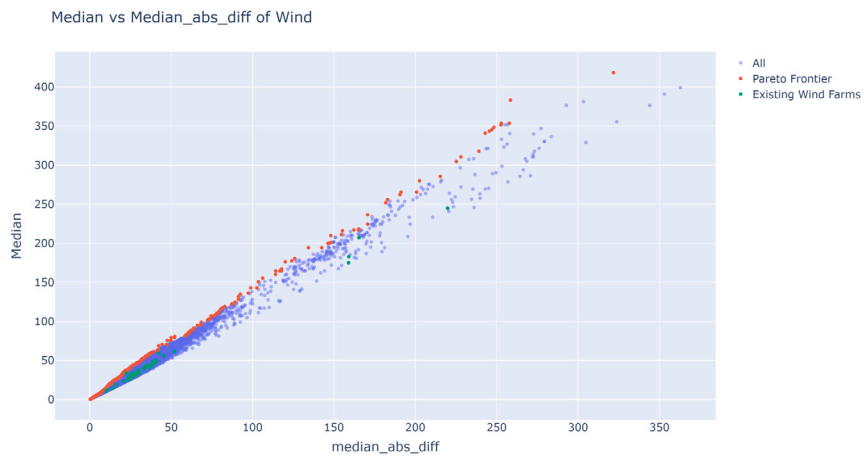
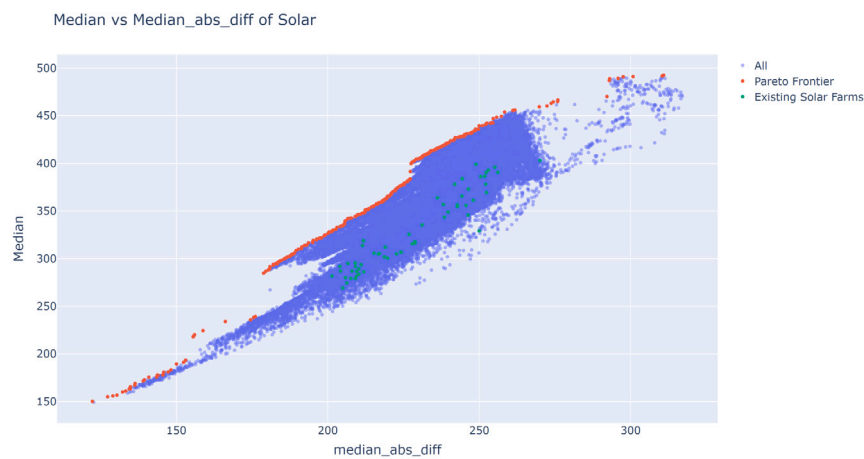


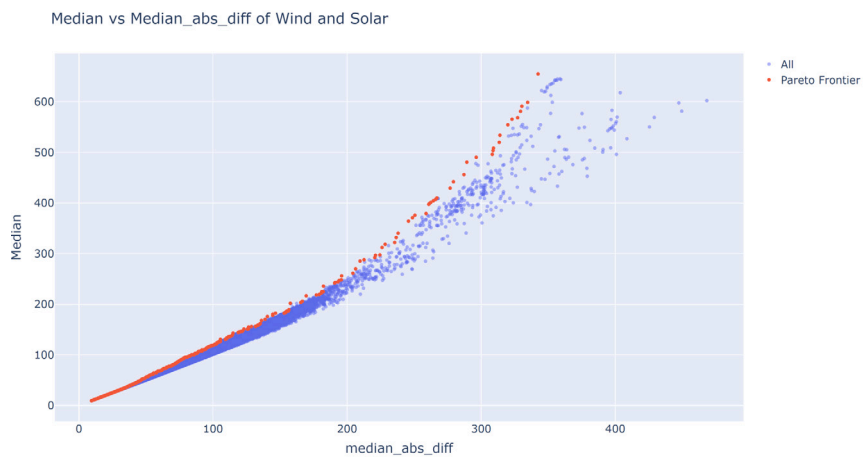
Fig. 5. RCoV of solar, wind, and combination of wind and solar.



(a) Wind



(b) Solar



(c) Wind and Solar

**Fig. 6.** Scatterplot of all median vs. median absolute difference of (a) wind, (b) solar and (c) combination of wind and solar power for all locations. Pareto-optimal sites are shown in red, existing wind and solar farms are shown in green.

Pareto frontiers of wind are more geographically dispersed and mainly located along eastern, western and southern coastline and Central West and South West of Queensland. The Pareto frontiers of wind and solar show a similar pattern as found in wind, which indicates that wind plays a major role when considering of wind and solar synergy in Australia. It is worth noting that the Pareto-

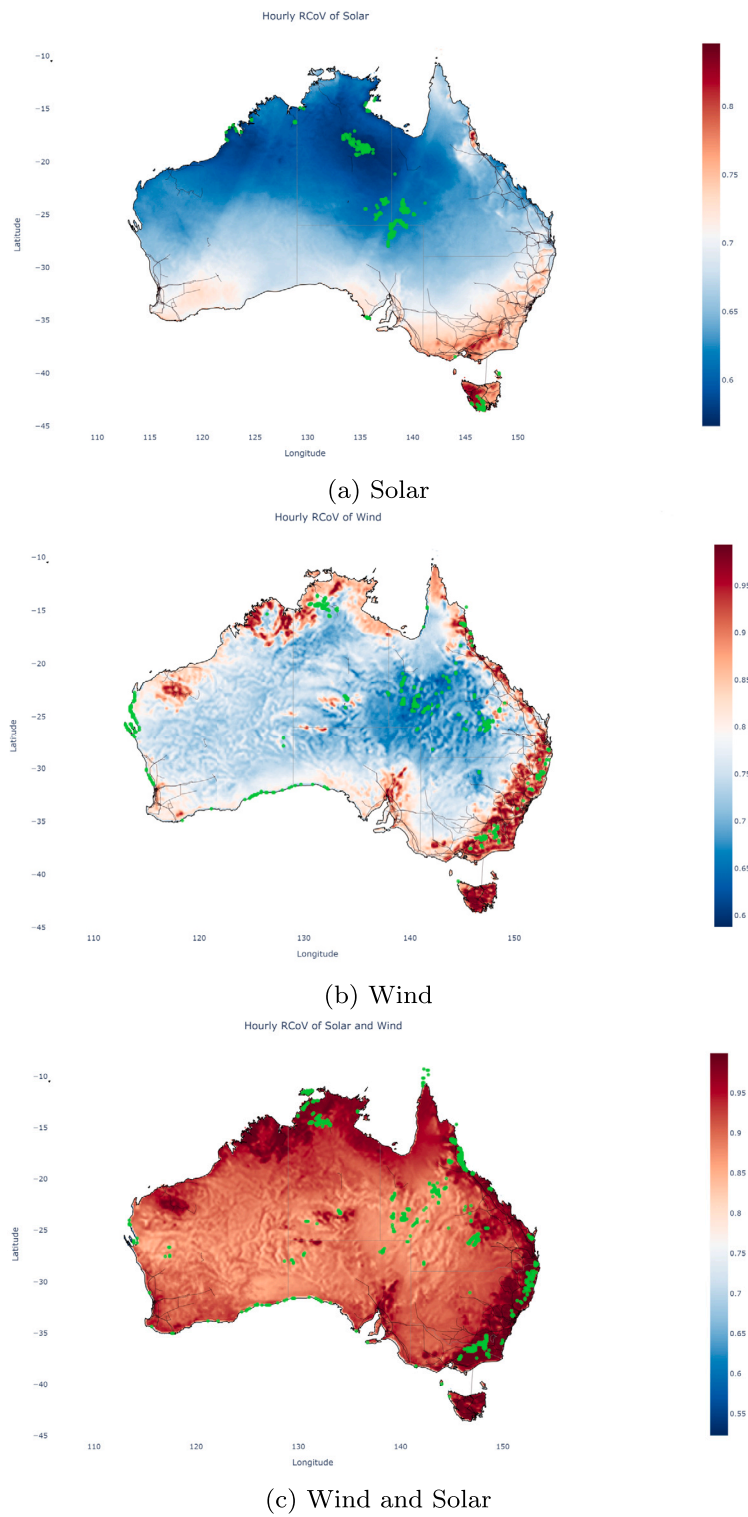


**Fig. 7.** RCoV of (a) solar, (b) wind and (c) combination of wind and solar in Australia with Pareto frontier points in green.

front locations shown include low-variability but low-energy locations, as shown on the lower left corners of Fig. 6. This results in some unlikely locations, such as solar farms in southern Tasmania, being shown for the sake of completeness. Commercial viability of such locations should obviously be assessed further. Fig. 7 gives an overall view of optimal wind, solar sites and co-optimisation

of wind and solar in Australia, some of these locations, however, are remote and not in the proximity of transmission infrastructure. Therefore, the optimisation problem will be further analysed for Renewable Energy Zones in next section.

### 3.3. RCoV of solar, wind, combination of solar and wind in renewable energy zones

As suggested by the preceding figures, the power output can be optimised when we select sites on Pareto frontier. However, the Pareto frontier was calculated based on all grid points in Australia. It is not economically feasible to select any sites suggested by the Pareto frontier when we plan to develop a new solar/wind farm since the locations on Pareto frontier could be remote and inaccessible, or far from transmission and population centres. Helpfully, the Integrated System Plan (ISP) by the Australian Energy Market Operator (AEMO) [20], proposes numerous Renewable Energy Zones (REZs) in the National Energy Market (NEM), as shown in Fig. 8. The NEM interconnects five regional market jurisdictions including Queensland, New South Wales (including Australian Capital Territory), Victoria, South Australia, and Tasmania. Since the REZs are being established in what was considered the most suitable locations for new renewable generation to the existing electricity infrastructure, we have focused our investigations to locations within the REZs. We note that this methodology pairs real sites with pareto-front sites from any location in any REZ, and so intentionally ignores additional constraints (e.g. transmission losses, interconnector limits, land-use concerns), to simplify the analysis and demonstrate an upper bound on the improvements from careful site selection if a hypothetical renewable grid were constructed from scratch. Real world limitations when selecting new renewable generation sites would almost certainly result in lower gains than presented in this section, but as our purpose is to demonstrate the utility of this analytical approach to planning new sites, comparing gains to existing generators remains a useful initial metric.

The Pareto frontiers of wind, solar, and wind plus solar in REZs are calculated, identified and presented in Fig. 9. The first map of Fig. 9 shows the sites on Pareto frontier of solar in REZs and existing solar farms in NEM. It is clear that in South Australia, the best sites are located in all REZs except for S2, S3 and S5. REZs' T2 in north-west Tasmania has much potential for solar generation. There is only one spot identified in New South Wales and it's N5 located on New South Wales and South Australia border. The best sites in Queensland are Q2, Q4, Q6 and Q7. Existing solar farms are all located within or in close proximity to the REZs. In the second map of 9, it can be observed that the sites on Pareto frontier for wind are more dispersed and they are identified in almost all REZs, which means there are more location options if wind farm is to be developed in those areas. The third map shows the best locations if we consider co-located projects of wind and solar. Sites on Pareto frontier can be mainly found in Queensland, N7 in New South Wales, V6 in Victoria and along the coastline of South Australia.

To evaluate the potential of this pareto front tool in making better site selections as compared to the incumbent industry processes, existing solar farm locations (shown as grey dots in Fig. 9) are paired with the sites on the pareto front in REZs with the same variability, and differences of the median output are calculated and presented in Table 2. The table lists the solar farms, their statistics, their paired grid points and the difference in the median. For instance, Bolivar Waste Water Treatment Plant solar farm is compared to a site with latitude  $-19.63$  and longitude  $142.61$ , which is Croydon Shire in Q2, Queensland. For these two site, the variability is similar, but the median output of the Pareto front site is  $82.3 \text{ W/m}^2$  (25%) higher. This indicates that if we had developed a solar farm at the proposed site instead of the current site, it would have generated 25% more energy at the same intermittency level. The table shows the average increase for all paired grid points in energy resource is 9%, and ranges from 1-25%, with the same level of intermittency.

Similarly, statistics of paired wind farms sites are shown in Table 3. It's interesting to observe that the differences are smaller than that of solar, which means the improvement potential of the proposed wind farm locations is not as promising as for solar farms. However, the average percentage improvement 28% (and ranges from 0-54%), suggests that it would have generated 28% more energy on average at the same intermittency level if the wind farm sites are selected from Pareto frontier. The average of the differences between paired wind farms is  $10.48 \text{ W/m}^2$ . The boxplots of median and median absolute deviation from median to compare between existing and proposed farms are presented in Fig. 10.

In Australia, Wind and solar have been paired in various off-grid locations, but the large-scale development of wind-solar hybrid plant meets obstacles and makes slow progress. There are currently 3 projects which can be considered as hybrid wind-solar plants. The Gullen Range solar farm south of Crookwell in New South Wales is the first large-scale solar farm on Australia's main grid to be co-located with a major wind farm. The Port Augusta Renewable Energy Park is a hybrid wind-solar plant and is located southeast of Port Augusta in South Australia. Kennedy Energy Park is a wind, solar and storage hybrid power station approximately 290 km southwest of Townsville in Queensland. If we extend our approach to selecting better locations for hybrid of wind and solar plants in the NEM, we get 16%, 14% and 3% improvement for 3 hybrid plants respectively in median energy, or if we pair sites by median, 11%, 10% and 2% improvement in intermittency, as shown in Table 4.

The results of three tables indicate that there will be substantial improvement in terms of median energy or intermittency if we carefully select sites for solar, wind and hybrid plants on Pareto frontier.

### 3.4. RCoV of offshore wind and combination of wind and solar

In the past few years, land is becoming a scarce resource at a global scale and the cost of acquiring land resources is soaring in Australia. For example, on the New England tablelands of New South Wales, developers are offering farmers up to \$30,000 per year for every turbine they host on their property in Walcha. The available spaces for new large scale wind and PV installations becomes limited and the interest has been turned into the marine environment. On the other hand, larger projects are more feasible offshore due to greater seabed areas available for development. Offshore wind speeds tend to be steadier and faster than on land,

**Table 2**  
A Comparison of Characteristics of Current and Proposed Solar Farms.

Solar Farms Station Name	Current Farms			Proposed Farms in REZs				Comparison	
	median	median_abs_diff	RCoV	Latitude	Longitude	median	median_abs_diff	median_diff	percentage improvement
Bolivar Waste Water Treatment Plant	329.16	249.99	0.76	-19.63	142.61	411.47	250.19	82.3	0.25
White Rock Wind and Solar Farm	345.69	246.33	0.71	-20.07	143.05	404.13	246.45	58.45	0.17
Yarranlea Solar Farm	355.88	245.62	0.69	-20.07	143.05	404.13	246.45	48.26	0.14
Gunnedah Solar Farm	343.47	238.53	0.69	-20.62	143.16	390.31	238.27	46.84	0.14
Oakey 1 Solar Farm	361.31	248.06	0.69	-19.96	142.72	407.28	246.95	45.97	0.13
Moree Solar Farm	348.89	239.7	0.69	-20.4	143.05	394.25	239.68	45.36	0.13
Gangarri Solar Farm	369.39	252.41	0.68	-19.3	142.61	414.55	253.16	45.16	0.12
Darling Downs Solar Farm	369.39	252.41	0.68	-19.3	142.61	414.55	253.16	45.16	0.12
Warwick Solar Farm 2	354.62	242.79	0.68	-20.29	143.05	398.41	242.4	43.79	0.12
Corowa Solar Farm	278.95	209.12	0.75	-29.86	136.56	317.05	209.07	38.11	0.14
Winton Solar Farm	269.13	204.94	0.76	-32.28	141.62	305.84	205.39	36.72	0.14
Glenrowan West Solar Farm	269.13	204.94	0.76	-32.28	141.62	305.84	205.39	36.72	0.14
Western Downs Green Power Hub	365.61	244.3	0.67	-20.07	142.72	402.13	244.28	36.52	0.1
Ross River Solar Farm	378.13	252.18	0.67	-19.74	142.61	414.5	251.61	36.38	0.1
Gullen Range Solar Farm	274.28	206.27	0.75	-31.73	140.85	310.17	206.34	35.89	0.13
Wagga North Solar Farm	281.32	209.4	0.74	-29.86	136.56	317.05	209.07	35.73	0.13
Bomen Solar Farm	281.32	209.4	0.74	-29.86	136.56	317.05	209.07	35.73	0.13
Mannum - Adelaide Pipeline Pumping Station	286.04	211.85	0.74	-31.07	141.84	321.54	211.68	35.5	0.12
Parkes Solar Farm	300.45	219.75	0.73	-30.08	138.76	335.08	219.44	34.63	0.12
Molong Solar Farm	304.94	222.67	0.73	-30.19	138.76	339.5	222.29	34.56	0.11
Sebastopol Solar Farm	283.55	210.27	0.74	-31.4	141.07	317.92	210.75	34.38	0.12
Junee Solar Farm	279.11	207.63	0.74	-31.51	140.85	313.09	207.7	33.98	0.12
Manildra solar Farm	306.64	224.25	0.73	-30.3	138.76	340.41	224.25	33.77	0.11
Goonumbla Solar Farm	306.74	224.13	0.73	-30.3	138.76	340.41	224.25	33.66	0.11
Suntop Solar Farm	316.36	228.84	0.72	-30.08	139.09	349.75	228.3	33.39	0.11
Childers Solar Farm	356.92	238.16	0.67	-20.62	143.16	390.31	238.27	33.39	0.09
Jemalong Solar Project	301.78	218.69	0.72	-30.08	138.76	335.08	219.44	33.3	0.11
Beryl Solar Farm	317.66	228.79	0.72	-30.08	139.09	349.75	228.3	32.09	0.1
Wellington Solar Farm	315.62	227.88	0.72	-29.97	139.2	347.23	227.61	31.62	0.1
Finley Solar Farm	286.47	209.53	0.73	-29.97	136.67	317.75	209.75	31.28	0.11
Haughton Solar Farm	373.09	246.44	0.66	-20.07	143.05	404.13	246.45	31.04	0.08
Adelaide Desalination Plant	289.03	210.23	0.73	-29.97	136.67	317.75	209.75	28.72	0.1
Bannerton Solar Park	304.89	216.68	0.71	-29.97	138.87	333	216.78	28.11	0.09
Lilyvale Solar Farm	386.48	251.84	0.65	-19.74	142.61	414.5	251.61	28.02	0.07
Wemen Solar Farm	305.13	217.06	0.71	-29.97	138.87	333	216.78	27.88	0.09
Darlington Point Solar Farm	293.55	210.98	0.72	-29.86	136.67	320.39	210.89	26.84	0.09
Numurkah Solar Farm	279.98	205.87	0.74	-32.28	141.73	306.58	205.75	26.6	0.1
Gannawarra Solar Farm	286.86	208.05	0.73	-31.51	140.85	313.09	207.7	26.23	0.09
Middlemount Solar Farm	386.19	250.52	0.65	-19.52	142.5	412.19	250.66	26	0.07
Susan River Solar Farm	363.88	236.23	0.65	-20.51	143.05	389.38	236.48	25.5	0.07
Coleambally Solar Farm	291.67	209.14	0.72	-29.86	136.56	317.05	209.07	25.38	0.09
Emerald Solar Park	390.5	252.3	0.65	-19.74	142.61	414.5	251.61	24	0.06
Clermont Solar Farm	390.64	256.14	0.66	-19.08	143.05	414.55	257.44	23.91	0.06
Bungala One Solar Farm	312	218.98	0.7	-30.08	138.76	335.08	219.44	23.08	0.07
Nevertire Solar Farm	325.47	226.83	0.7	-29.97	139.2	347.23	227.61	21.77	0.07
Rugby Run Solar Farm	392.86	252.98	0.64	-19.3	142.61	414.55	253.16	21.69	0.06
Limondale Solar Farm	295.45	209.09	0.71	-29.86	136.56	317.05	209.07	21.6	0.07
Sunraysia Solar Farm	295.45	209.09	0.71	-29.86	136.56	317.05	209.07	21.6	0.07
Limondale Solar Farm	295.45	209.09	0.71	-29.86	136.56	317.05	209.07	21.6	0.07
Hillston Sun Farm	305.73	215.26	0.7	-30.41	137.22	325.55	215.11	19.82	0.06
Kidston Solar Project	403.19	270.05	0.67	-18.86	143.27	422.8	266.39	19.61	0.05
Kennedy Energy Park Solar	396.05	255.16	0.64	-19.3	142.61	414.55	253.16	18.5	0.05
Whitsunday Solar Farm	383.99	244.4	0.64	-20.07	142.72	402.13	244.28	18.13	0.05
Hamilton Solar Farm	383.99	244.4	0.64	-20.07	142.72	402.13	244.28	18.13	0.05
Hayman Solar Farm	383.99	244.4	0.64	-20.07	142.72	402.13	244.28	18.13	0.05
Collinsville Solar PV Power Station	383.99	244.4	0.64	-20.07	142.72	402.13	244.28	18.13	0.05
Daydream Solar Farm	383.99	244.4	0.64	-20.07	142.72	402.13	244.28	18.13	0.05
Maryrorough Solar Farm	378.02	241.92	0.64	-20.73	143.38	395.84	241.92	17.83	0.05
Clare Solar Farm	378.02	241.92	0.64	-20.73	143.38	395.84	241.92	17.83	0.05
Nyngan Solar Plant	335.38	231.14	0.69	-30.52	139.31	352.39	232.17	17.02	0.05
Kiamal Solar Farm	286.91	204.22	0.71	-32.39	141.62	303.15	204.18	16.24	0.06
Karadoc Solar Farm	294.97	206.63	0.7	-31.73	140.85	310.17	206.34	15.2	0.05
Yatpool Solar Farm	291.7	204.03	0.7	-32.39	141.62	303.15	204.18	11.45	0.04
Sun Metals Solar Farm	399.02	248.91	0.62	-19.96	143.05	407.7	249.45	8.69	0.02
Broken Hill Solar Plant	313.87	211.49	0.67	-31.07	141.84	321.54	211.68	7.67	0.02
Tailem Bend Solar Project	281.7	201.36	0.71	-34.04	138.1	289.16	202.2	7.45	0.03
Morgan-Whyalla Pipeline Pumping Station	318.84	211.75	0.66	-31.07	141.84	321.54	211.68	2.7	0.01
								29.19	0.09

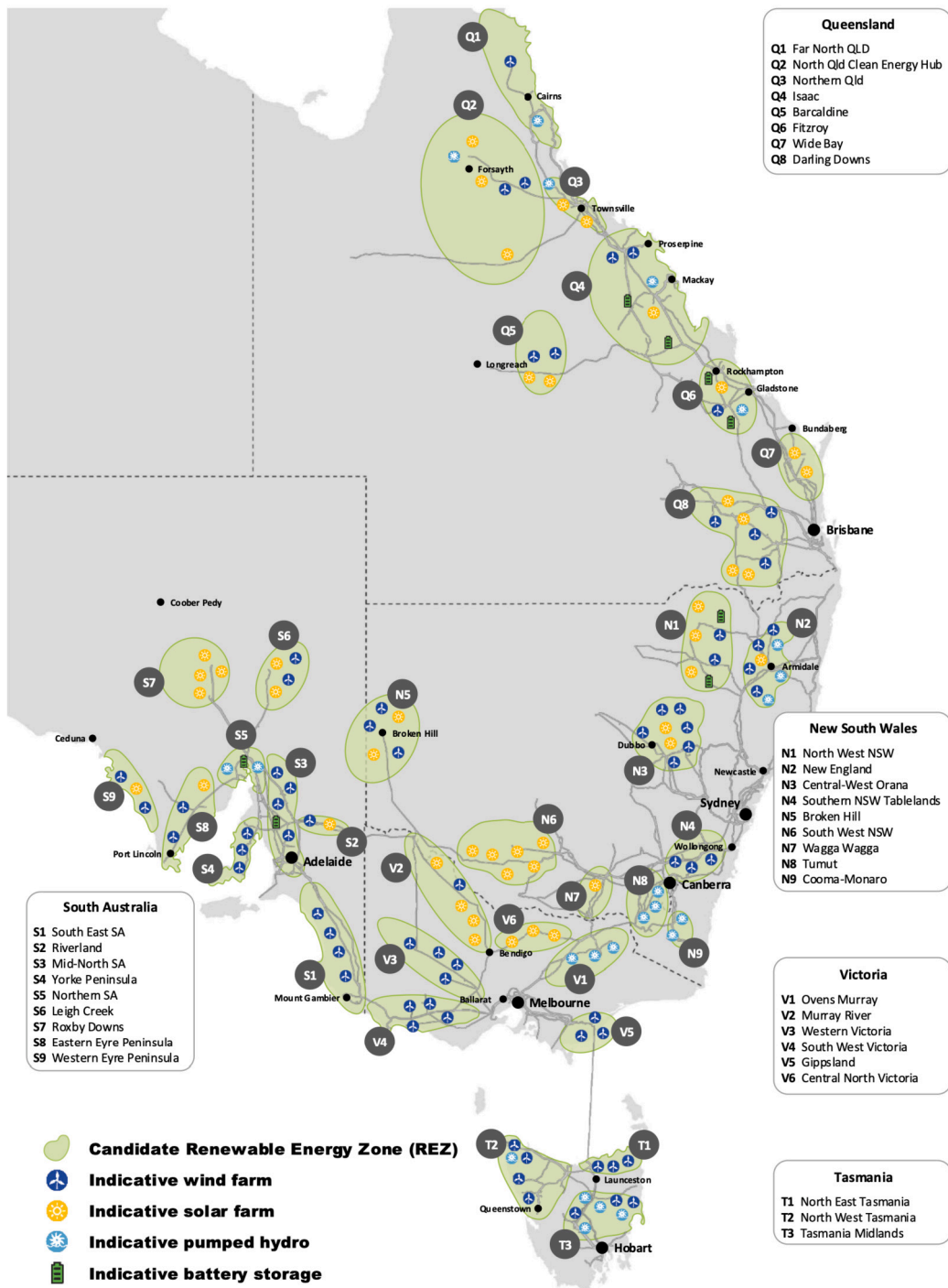
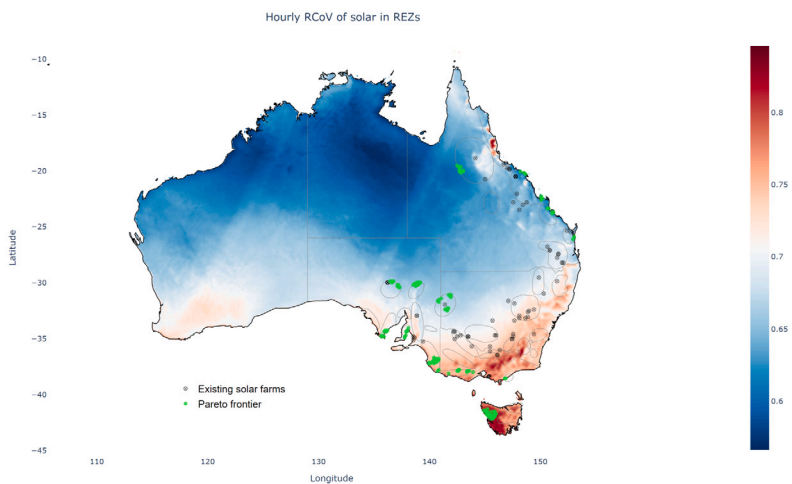
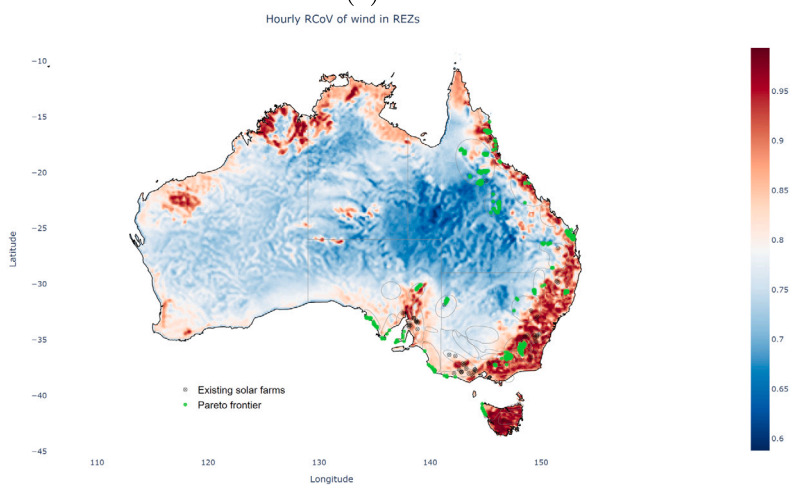


Fig. 8. Renewable Energy Zones.

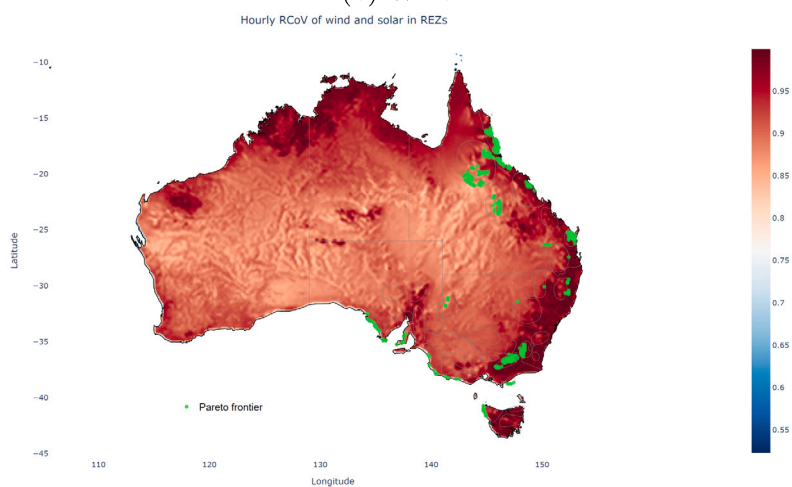
and even small increases in speed can produce large increase in energy generation, which means a more reliable source of energy. Therefore, offshore wind is booming globally with the International Energy Agency viewing offshore wind as one of the big three sources of clean energy alongside solar and onshore wind. Offshore solar energy has been studied by [21] as a standalone form of renewable energy resource in the coastal and offshore environment during the last few years. While the potential for offshore resources in Australia has been overlooked for some time, it is believed that Australia could be a global offshore wind superpower as the wind resources are among the world's best, see [22]. With the development of both fixed and floating offshore wind turbines, the



(a) Solar



(b) Wind



(c) Wind and Solar

**Fig. 9.** Pareto frontier of (a) solar, (b) wind and (c) combination of solar and wind resource in renewable energy zones. Pareto-front locations shown as green dots. Existing solar and wind farms shown as grey dots.

**Table 3**  
A Comparison of Characteristics of Current and Proposed Wind Farms.

Wind Farms				Proposed Farms in REZs				Comparison	
Station Name	median	median_abs_diff	RCoV	Latitude	Longitude	median	median_abs_diff	median_diff	percentage improvement
Musselroe Wind Farm	175.07	159	0.91	-37.78	140.41	207.08	165.44	32.01	0.18
Bald Hills Wind Farm	182.78	159.19	0.87	-37.78	140.41	207.08	165.44	24.3	0.13
Gunning Wind Farm	40.88	36.73	0.9	-20.95	144.48	57.7	36.77	16.82	0.41
Ararat Wind Farm	42.93	37.57	0.88	-20.95	144.37	59.21	38.18	16.27	0.38
Mt Mercer Wind Farm	43.94	38.06	0.87	-20.95	144.37	59.21	38.18	15.26	0.35
Granville Harbour Wind Farm	244.95	219.84	0.9	-39.54	144.15	260.12	215.64	15.17	0.06
Willogeleche Wind Farm	43.05	36.2	0.84	-20.95	144.48	57.7	36.77	14.65	0.34
North Brown Hill Wind Farm	43.23	36.22	0.84	-20.95	144.48	57.7	36.77	14.47	0.33
Crookwell 2 Wind Farm	45.14	39.17	0.87	-20.95	144.26	59.47	39.45	14.33	0.32
Cattle Hill Wind Farm	25.96	24.96	0.96	-18.42	144.92	39.95	25.23	13.99	0.54
Crowlands Wind Farm	25.51	23.84	0.93	-18.31	144.92	39.26	24.2	13.75	0.54
Bango 999 Wind Farm	32.35	29.31	0.91	-21.06	144.59	45.93	29.69	13.57	0.42
Gullen Range Wind Farm	33.82	30.51	0.9	-19.96	144.37	47.26	30.55	13.44	0.40
Woodlawn Wind Farm	25.86	24.19	0.94	-18.31	144.92	39.26	24.2	13.4	0.52
Snowtown Wind Farm	34.04	30.45	0.89	-19.96	144.37	47.26	30.55	13.23	0.39
Snowtown South Wind Farm	43.53	35.18	0.81	-20.84	144.48	56.4	35.34	12.87	0.30
Hallett 1 Wind Farm	38.4	33.24	0.87	-21.06	143.82	50.54	33.31	12.14	0.32
The Bluff Wind Farm	38.4	33.24	0.87	-21.06	143.82	50.54	33.31	12.14	0.32
Bodangora Wind Farm	28.09	24.86	0.88	-18.42	144.92	39.95	25.23	11.86	0.42
Lincoln Gap Wind Farm	29.54	27.07	0.92	-22.6	145.69	41.34	27.46	11.8	0.40
Moorabool Wind Farm	47.88	40.47	0.85	-18.31	144.81	59.6	40.51	11.73	0.24
Collector Wind Farm 1	29.65	27.13	0.92	-22.6	145.69	41.34	27.46	11.7	0.39
Hornsedale Wind Farm	34.53	29.11	0.84	-21.06	144.59	45.93	29.69	11.39	0.33
Waterloo Wind Farm	47.88	38.59	0.81	-20.95	144.37	59.21	38.18	11.33	0.24
Bulgana Green Power Hub	33.16	28.5	0.86	-21.94	145.69	44.48	28.41	11.31	0.34
Stockyard Hill Wind Farm	49.23	40.99	0.83	-18.31	144.81	59.6	40.51	10.37	0.21
Clements Gap Wind Farm	42.05	34.01	0.81	-21.06	144.48	52.3	34.01	10.25	0.24
Snowtown Wind Farm	40.12	33.11	0.83	-21.94	145.58	50.04	33.07	9.92	0.25
Mount Emerald Wind Farm	23.55	21.19	0.9	-22.71	146.13	33.16	21.44	9.62	0.41
Macarthur Wind Farm	50.04	40.76	0.81	-18.31	144.81	59.6	40.51	9.56	0.19
Oaklands Hill Wind Farm	41.17	33.73	0.82	-22.16	145.58	50.54	33.76	9.37	0.23
Mt Gellibrand Wind Farm	23.35	20.7	0.89	-22.82	146.24	32.57	20.46	9.22	0.39
Coopers Gap Wind Farm	30.8	25.29	0.82	-18.42	144.92	39.95	25.23	9.14	0.30
Salt Creek Wind Farm	28.09	23.61	0.84	-19.96	144.59	37.04	23.46	8.95	0.32
Dundonnell Wind Farm	28.09	23.61	0.84	-19.96	144.59	37.04	23.46	8.95	0.32
Murra Warra Wind Farm	37.83	30.03	0.79	-21.06	144.59	45.93	29.69	8.1	0.21
Taralga Wind Farm	33.65	26.94	0.8	-23.26	145.69	41.29	26.69	7.63	0.23
Kiata Wind Farm	32.35	24.92	0.77	-18.42	144.92	39.95	25.23	7.6	0.23
Crudine Ridge Wind Farm	14.93	14.48	0.97	-18.42	145.03	21.64	14.51	6.71	0.45
Bango 973 Wind Farm	14.27	14.03	0.98	-32.28	147.01	19.82	14.05	5.56	0.39
Yendon Wind Farm	55.81	45.33	0.81	-31.51	141.4	61.19	45.13	5.38	0.10
Elaine Wind Farm	55.81	45.33	0.81	-31.51	141.4	61.19	45.13	5.38	0.10
White Rock Wind and Solar Farm	19.1	16.21	0.85	-23.59	146.13	24.33	15.91	5.23	0.27
Berrybank Wind Farm	61.66	51.91	0.84	-34.81	137.55	66.05	51.87	4.39	0.07
Boco Rock Wind Farm	10.78	10.33	0.96	-18.31	143.16	13.86	10.35	3.08	0.29
Sapphire Wind Farm	12.46	10.69	0.86	-18.31	143.05	14.72	10.68	2.26	0.18
Cherry Tree Wind Farm	10.48	10.02	0.96	-28.54	151.19	12.62	9.99	2.14	0.20
Silverton Wind Farm	59.47	42.51	0.71	-31.4	141.62	60.66	43.26	1.19	0.02
Kennedy Energy Park Wind	33.65	22.54	0.67	-22.82	146.13	34.53	22.38	0.88	0.03
Lake Bonney Stage 2 Windfarm	207.08	165.44	0.8	-37.78	140.41	207.08	165.44	0	0.00
								10.48	0.28

offshore wind farms can be integrated to the grid to achieve diversity of supply, high capacity factor and employment opportunities. Therefore, the potential for offshore resources must be reconsidered.

In this section, the potential of offshore renewable energy resources are studied in Australia’s exclusive economic zone. An exclusive economic zone (EEZ), as prescribed by the 1982 United Nations Convention on the Law of the Sea, is an area of the sea in which a sovereign state has special rights regarding the exploration and use of marine resources, including energy production from water, wind and solar.

The scatterplot of median and median absolute difference of wind is illustrated in Fig. 11 and the RCoV of wind power density in the EEZ is shown in Fig. 12. There are two clusters in the scatterplot, one at latitude -10 to -25 and the other at latitude -35 to -45. The group close to Equator has smaller median and median absolute difference than the group further south. The profile of wind RCoV is not very varied with the range from 0.6 to 0.95. There are 705 grid points on Pareto frontier in total but most of them are at a distance of more than 100 km from the coastline which makes it impractical to develop offshore wind farms. Therefore, only

**Table 4**  
Statistics of selected grid points (Wind and Solar).

Station Name	Latitude	Longitude	median	median_abs_diff	% improvement
Gullen Range Wind Farm	-34.62	149.46	123.42	116.77	
Port Augusta Renewable Energy Park	-32.34	137.51	101.94	97.66	
Kennedy Energy Park	-21.00	145.00	86.05	76.87	
Paired by median_abs_diff	-18.31	144.81	142.95	114.96	0.16
	-20.95	143.82	115.90	98.97	0.14
	-22.82	146.24	89.01	76.55	0.03
Paired by median	-21.06	143.93	122.77	103.54	0.11
	-23.37	145.69	101.84	88.27	0.10
	-23.37	146.24	86.08	75.19	0.02

**Table 5**  
Statistics of selected grid points (offshore wind).

	latitude	longitude	median( $W/m^2$ )	median_absd( $W/m^2$ )	RCoV
1	-19.735	147.995	126.317	86.368	0.684
2	-19.625	147.775	179.719	125.128	0.696
3	-19.515	147.665	108.366	70.495	0.651
4	-19.185	147.225	152.146	109.922	0.722
5	-15.445	145.355	149.357	102.338	0.685
6	-15.445	145.465	483.305	344.757	0.713
7	-14.785	145.355	428.675	293.828	0.685
8	-14.785	145.575	371.889	250.976	0.675
9	-14.785	145.685	363.171	246.647	0.679
10	-14.675	145.025	130.324	86.382	0.663
11	-14.675	145.135	316.591	208.688	0.659
12	-14.675	145.245	448.581	301.104	0.671
13	-14.675	145.355	423.968	288.849	0.681
14	-14.675	145.465	383.251	258.458	0.674
15	-14.675	145.575	376.274	253.166	0.673

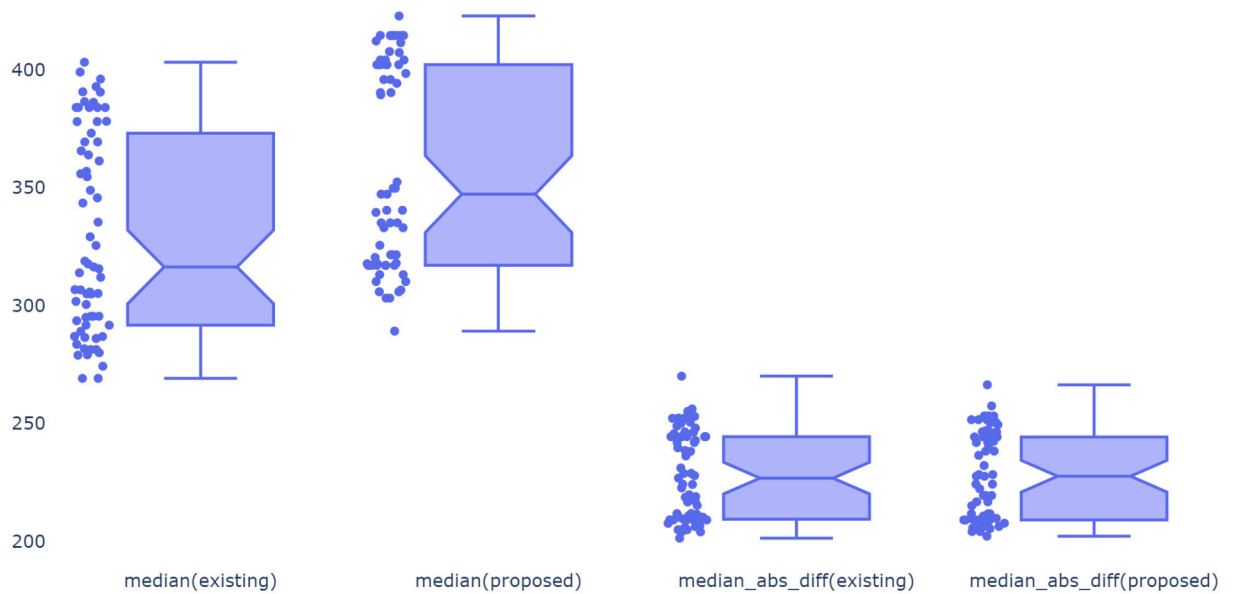
**Table 6**  
Statistics of selected grid points (offshore wind and solar).

	latitude	longitude	median_inst( $W/m^2$ )	median_absd( $W/m^2$ )	RCoV
1	-15.445	145.465	783.43	396.86	0.51
2	-34.585	136.005	252.50	206.15	0.82
3	-25.125	152.835	221.59	185.79	0.84
4	-40.965	145.905	175.94	148.87	0.85
5	-19.955	148.325	167.93	143.60	0.86
6	-22.155	149.645	164.49	141.80	0.86
7	-24.025	151.845	160.08	140.71	0.88
8	-23.805	151.405	159.51	140.64	0.88
9	-41.075	146.235	145.82	128.93	0.88
10	-27.215	153.165	142.95	125.71	0.88
11	-24.575	152.285	142.48	122.66	0.86
12	-25.015	152.615	132.73	114.04	0.86
13	-26.555	153.165	127.00	111.27	0.88
14	-25.125	152.725	117.77	101.15	0.86

grid points within 100 km of transmission infrastructures and their median larger than  $100 W/m^2$  are considered. 15 grid points are identified near Cooktown in Queensland and they are shown in Fig. 12 in green and their statistics are shown in Table 5.

As solar power has become much cheaper in recent years, offshore solar is another option for new electricity power plants. Floating solar panels has been placed on reservoirs around the world in various projects. Offshore solar is challenging but research and testing are undertaken to ensure that solar panels work in rough water. For example, Dutch-Norwegian company SolarDuck’s offshore floating solar plant is due to be operational in 2026. As it is very likely that offshore solar farm will use the existing cabling for the offshore wind farm to send electricity back to the shore, co-location of wind and solar should be considered for offshore projects as well. Similar analysis was conducted for combination of wind and solar and their statistics are shown in Table 6. The scatterplot of median and median absolute difference of wind and solar at each grid point is illustrated in Fig. 13 and the RCoV of wind and solar in EEZs is shown in Fig. 13. The RCoV values of wind and solar are varied with range from 0.5 to 0.95 and there are also two clusters in the scatterplot and the spread of the points are wider than that of wind alone, which indicates that it can benefit more from selecting grid points on Pareto frontier. The points in northern and northwest regions are generally have higher RCoV, and those in west and northeast regions have lower RCoV. Under the condition of within 50 km of transmission line and median

### A comparison between existing and proposed solar farms



### A comparison between existing and proposed wind farms

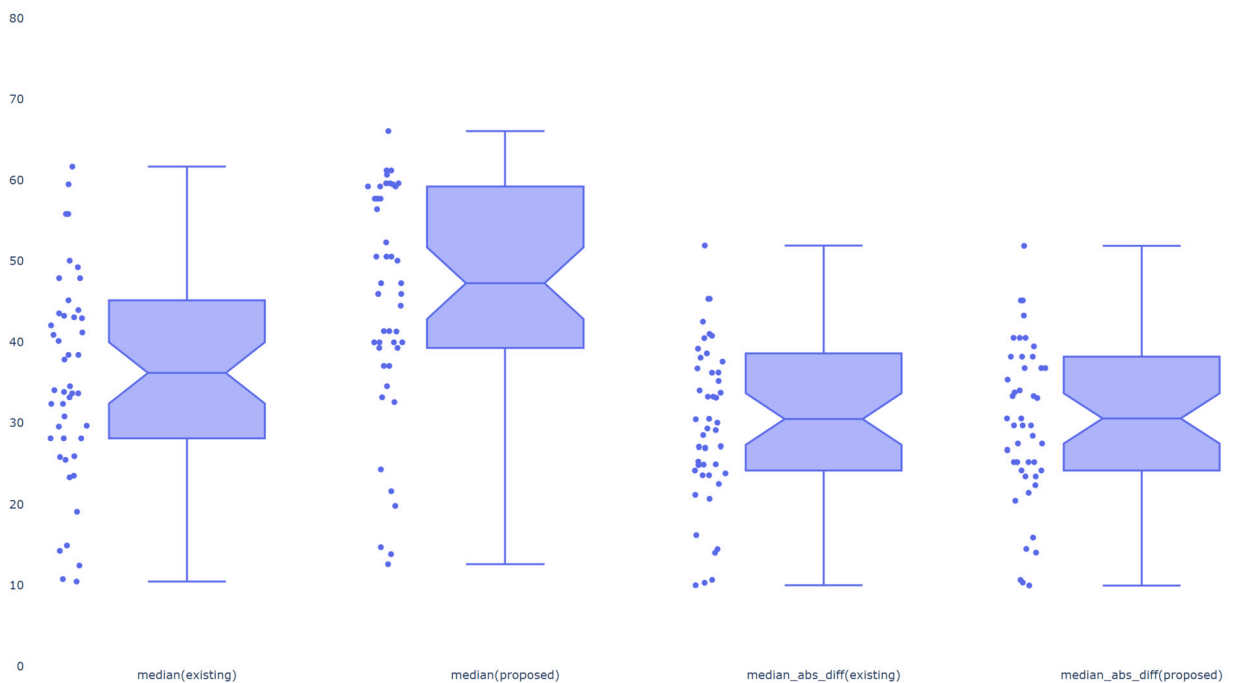


**Fig. 10.** A comparison of the energy (median), and intermittency (mean absolute difference) between existing and proposed farms.

larger than  $100 W/m^2$ , there are 14 grid points identified on Pareto frontier. They are located along east coast and to the north of Tasmania and marked in green in Fig. 14.

#### 4. Conclusion

In this study, the wind and solar power have been analysed based on the BARRA reanalysis dataset of Australia. Various correlation coefficients have been discussed and Kendall's  $\tau$  has been employed to assess wind and solar's correlation. WCS, SCW, WSS and RCoV

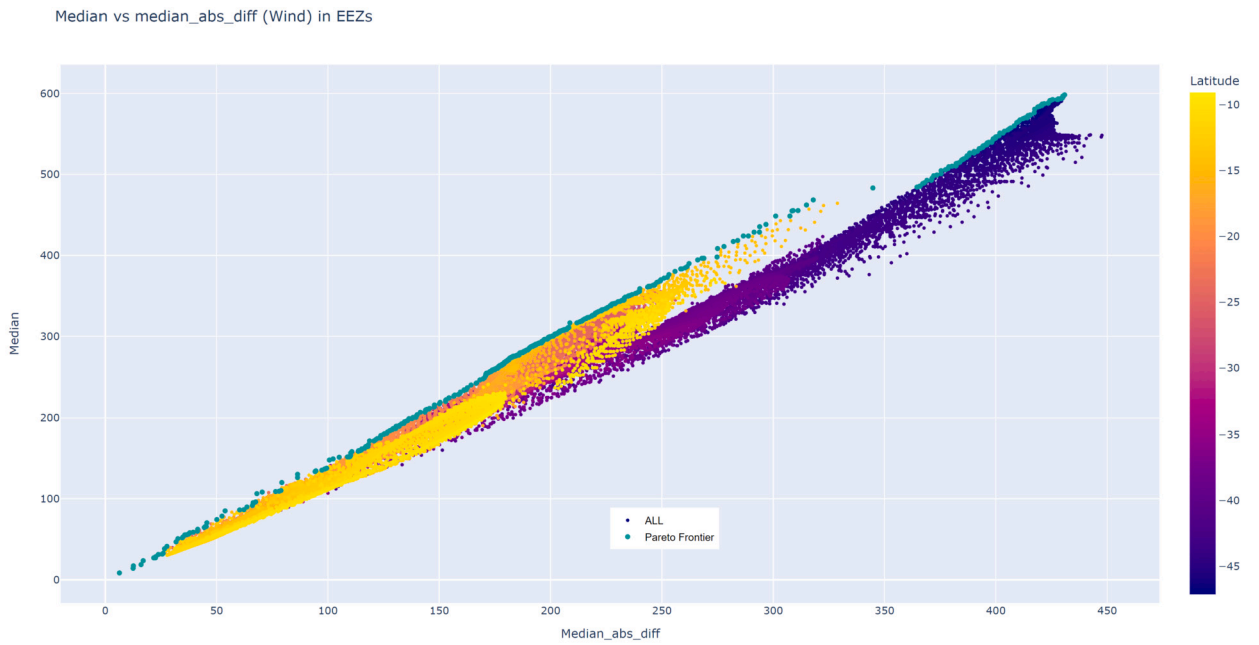


Fig. 11. Pareto frontier of wind resource in exclusive economic zones. Points are coloured by latitude to help distinguish their location.

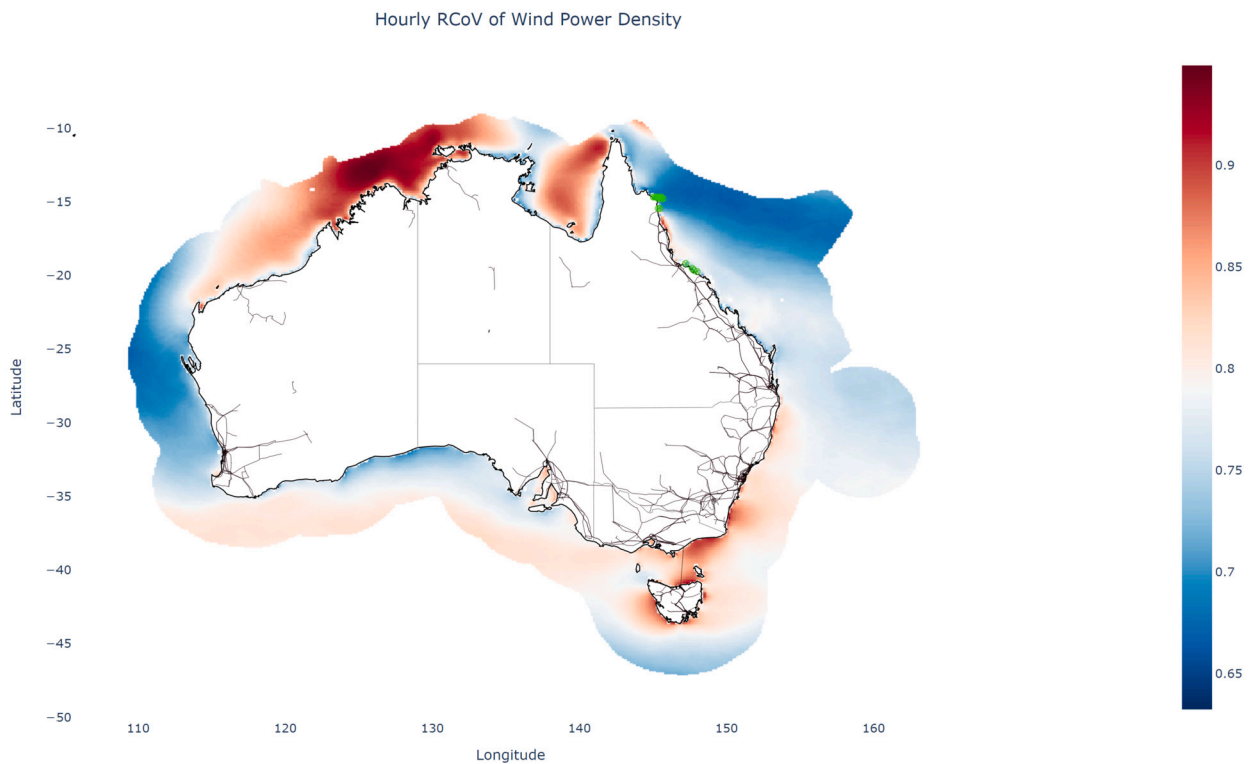


Fig. 12. RCoV of wind resource in exclusive economic zones. Green dots show the best 15 sites (lowest RCoV).

have been adopted to analyse wind and solar complementarity. In general, northern Australia, south-eastern and south-western coastal region and eastern Tasmania show strong negative correlation of wind and solar output on longer time scales based on Kendall's Tau. Western, south-western and southern coastal areas see greater availability of WCS while northern and eastern regions show higher SCW. The western and southern coastal regions are better locations in terms of WSS. Since the distribution of wind speed is highly skewed, RCoV is utilised to assess the variability of wind and solar resources, separately and jointly. RCoV shows



Fig. 13. Pareto frontier of wind and solar resource in exclusive economic zones. Points are coloured by latitude to help distinguish their location.

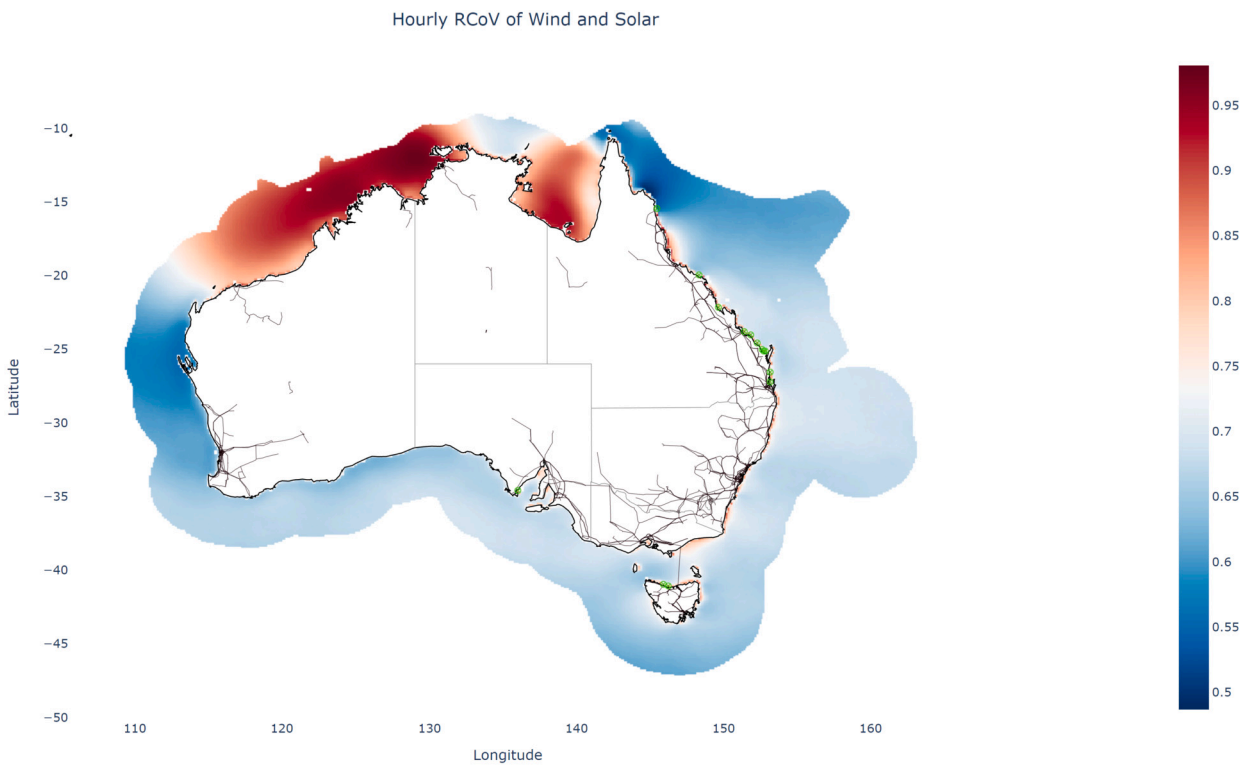


Fig. 14. RCoV of wind and solar resource in exclusive economic zones. Green dots show the best 15 sites (lowest RCoV).

the extend of variability in relation to the median, therefore, it can be considered as a standardised variability. However, the site selection process is a multi-objective optimisation and a trade-off between median and variance should be taken into consideration. Therefore, the Pareto frontier approach has been proposed to analyse the optimal profiles of wind, solar, and the combination of wind and solar. The results show that

- there will be on average 9% percentage improvement in median energy for solar and 28% for wind if we pair the existing farm with the grid points on Pareto frontier in REZs.
- there will be 3% to 16% improvement in median energy and 2% to 11% in intermittency for hybrid wind-solar project.

This analysis has also been extended to EEZs to identify the optimal sites offshore for wind and the combination of wind and solar. It has shown that our approach not only helps identify the location of optimal sites but also statistically quantifies the improvement. It can be useful to assess wind and solar resource and projects in Western Australia when the data are made available. While these results have been generated only on the Australian continent in this paper, the proposed bi-objective metric for selecting the best sites for wind and solar generation on the basis of both energy and intermittency is applicable worldwide, and universally important for maximising the effectiveness of the rapid rollout of renewable generation required for net-zero targets.

### CRedit authorship contribution statement

**Hao Wu:** Writing – original draft, Visualization, Resources, Project administration, Methodology, Investigation, Formal analysis, Data curation, Conceptualization. **Samuel R. West:** Writing – review & editing, Validation, Supervision, Software, Project administration, Funding acquisition, Formal analysis, Data curation, Conceptualization.

### Declaration of competing interest

The authors declare the following financial interests/personal relationships which may be considered as potential competing interests:

Hao Wu reports financial support was provided by CSIRO Energy Centre Newcastle. Samuel R West reports a relationship with CSIRO Energy Centre Newcastle that includes: employment.

### Data availability

Data associated with our study is publicly available and can be assessed through <http://www.bom.gov.au/research/projects/reanalysis/>.

### Acknowledgement

This paper was produced as a research program supported by the Commonwealth Scientific and Industrial Research Organisation (CSIRO). The authors wish to thank Bureau of Meteorology Australia for providing the datasets.

### References

- [1] Guorui Ren, Jie Wan, Wei Wang, Jizhen Liu, Feng Hong, Daren Yu, Quantitative insights into the differences of variability and intermittency between wind and solar resources on spatial and temporal scales in China, *J. Renew. Sustain. Energy* 13 (4) (2021) 043307.
- [2] Franciele Weschenfelder, Gustavo de Novaes Pires Leite, Alexandre Carlos Araújo da Costa, Olga de Castro Vilela, Claudio Moises Ribeiro, Alvaro Antonio Villa Ochoa, Alex Maurício Araújo, A review on the complementarity between grid-connected solar and wind power systems, *J. Clean. Prod.* 257 (2020) 120617.
- [3] Joakim Widén, Correlations between large-scale solar and wind power in a future scenario for Sweden, *IEEE Trans. Sustain. Energy* 2 (2) (2011) 177–184.
- [4] S. Jerez, R.M. Trigo, A. Sarsa, R. Lorente-Plazas, D. Pozo-Vázquez, J.P. Montávez, Spatio-temporal complementarity between solar and wind power in the Iberian Peninsula, *Energy Proc.* 40 (2013) 48–57.
- [5] F. Monforti, T. Huld, K. Bódis, L. Vitali, M. D'isidoro, R. Lacal-Aránzategui, Assessing complementarity of wind and solar resources for energy production in Italy. A Monte Carlo approach, *Renew. Energy* 63 (2014) 576–586.
- [6] Philip E. Bett, Hazel E. Thornton, The climatological relationships between wind and solar energy supply in Britain, *Renew. Energy* 87 (2016) 96–110.
- [7] Mario Marcello Miglietta, Thomas Huld, Fabio Monforti-Ferrario, Local complementarity of wind and solar energy resources over Europe: an assessment study from a meteorological perspective, *J. Appl. Meteorol. Climatol.* 56 (1) (2017) 217–234.
- [8] Takvor T. Soukissian, Flora E. Karathanasi, Dimitrios K. Zaragkas, Exploiting offshore wind and solar resources in the Mediterranean using era5 reanalysis data, *Energy Convers. Manag.* 237 (2021) 114092.
- [9] Christina E. Hoicka, Ian H. Rowlands, Solar and wind resource complementarity: advancing options for renewable electricity integration in Ontario, Canada, *Renew. Energy* 36 (1) (2011) 97–107.
- [10] Joanna H. Slusarewicz, Daniel S. Cohan, Assessing solar and wind complementarity in Texas, *Renew.: Wind, Water, Sol.* 5 (1) (2018) 1–13.
- [11] Gilberto Pianezzola, Arno Krenzinger, Fausto A. Canales, Complementarity maps of wind and solar energy resources for Rio Grande do Sul, Brazil, *Energy Power Eng.* 9 (09) (2017) 489–504.
- [12] Yi Liu, LiYe Xiao, HaiFeng Wang, ShaoTao Dai, ZhiPing Qi, Analysis on the hourly spatiotemporal complementarities between China's solar and wind energy resources spreading in a wide area, *Sci. China, Technol. Sci.* 56 (2013) 683–692.
- [13] Lanjing Xu, Zhiwei Wang, Yanfeng Liu, The spatial and temporal variation features of wind-sun complementarity in China, *Energy Convers. Manag.* 154 (2017) 138–148.
- [14] Yi Li, Vassilios G. Agelidis, Yash Shrivastava, Wind-solar resource complementarity and its combined correlation with electricity load demand, in: 2009 4th IEEE Conference on Industrial Electronics and Applications, IEEE, 2009, pp. 3623–3628.
- [15] Abhnil A. Prasad, Robert A. Taylor, Merlinda Kay, Assessment of solar and wind resource synergy in Australia, *Appl. Energy* 190 (2017) 354–367.
- [16] Chun-Hsu Su, Nathan Eizenberg, Peter Steinle, Dörte Jakob, Paul Fox-Hughes, Christopher J. White, Susan Rennie, Charmaine Franklin, Intiaz Dharssi, Hongyan Zhu, Barra v1. 0: the bureau of meteorology atmospheric high-resolution regional reanalysis for Australia, *Geosci. Model Dev.* 12 (5) (2019) 2049–2068.
- [17] Ali Naci Celik, A statistical analysis of wind power density based on the Weibull and Rayleigh models at the southern region of Turkey, *Renew. Energy* 29 (4) (2004) 593–604.

- [18] Maisam Wahbah, Tarek H.M. El-Fouly, Bashar Zahawi, Samuel Feng, Hybrid beta-kde model for solar irradiance probability density estimation, *IEEE Trans. Sustain. Energy* 11 (2) (2019) 1110–1113.
- [19] Udaya Bhaskar Gunturu, C. Adam Schlosser, Characterization of wind power resource in the United States, *Atmos. Chem. Phys.* 12 (20) (2012) 9687–9702.
- [20] Australian Energy Market Operator, Integrated System Plan for the National Electricity Market, 2018.
- [21] Vinod Kumar, R.L. Shrivastava, S.P. Untawale, Solar energy: review of potential green & clean energy for coastal and offshore applications, *Aquat. Proc.* 4 (2015) 473–480.
- [22] Australian Trade, Investment Commission, et al., *Why Australia?*, Benchmark report, 2015, p. 2015.